Modelling and simulation of a hydraulic active heave compensation system

Arkadiusz Jakubowski[1,*], and *Arkadiusz* Kubacki[1]
[1]Institute of Mechanical Technology, Poznan University of Technology, Skłodowska-Curie Square 5, 60-965 Poznań, Poland

Abstract. The following work presents modelling, simulation and results of hydraulic motor and hydraulic cylinder position measurement for a hydraulic active heave compensation system (AHC). In order to perform experimental research the authors developed a test stand. A hydraulic cylinder is used to carry out a simulation of sea waves. The development of a test stand made it possible to compare the simulation with the experimental results. A hydraulic motor is used for compensation of sea waves. Optimization of design parameters for such systems can be done by analysing a model simulation. The main components of this system were modelled. This model was implemented in simulation software Mathlab Simulink and its dynamic performance was tested. The Authors presented the simulation and the experimental results for main components of a hydraulic active heave compensation system.

1 Introduction

An electrohydraulic servo-drive is used in many industrial applications. Hydraulic systems are well established in the marine industry. Hydraulic actuators provide the highest power to weight ratio of any actuator currently on the market. The electrohydraulic servo-drives can be controlled by two types of electro-valves: proportional and servo-valves. Basic information about electrohydraulic servo drives is found in [1] and [2].

The heave compensation unit is an extremely important piece of equipment. Drilling, load handling, observation of seabed during rough sea are difficult to execute. For this reason heave compensation systems are applied. There are three types of heave compensation: passive heave compensation (PHC), active heave compensation (AHC) and semi-active heave compensation (SAHC). The first two are more commonly used than the last one. In the last few years, both passive heave (PHC) and active heave (AHC) systems have been researched and developed in order to improve drilling and load handling on the ship during rough sea [3,4].

Examples of research on PHC systems include the work by Huster *et al.* who used a gas-backed accumulator as a spring for PHC [5]. Another work about PHC is by Kidera who found the solution to the problem of a cylinder stick where static friction was too large for the load. Hatleskog and Dunnigan researched passive heave systems and one of the conclusions they made was that the only way to reduce heave motion by over 80% is by using an active compensator [6]. In the active heave compensation systems, ship's heave motion is measured and sent to a controller which moves an actuator. In these systems hydraulic drivers such as a hydraulic motor and a hydraulic cylinder are used. Over the last few years the research focused on the development of a new control algorithm [7, 8]. Kyllingstad applied transfer function filters [9]. Another work about a new algorithm is by Kuchler et al. who used heave-prediction algorithms to predict heave motion [10].

Modelling of the AHC system can be divided into three main parts: control, hydraulic and mechanical system. In this work the Authors focused on a modelling hydraulic system. The hydraulic system consists of a hydraulic cylinder and a hydraulic motor which are controlled by two servo valves.

2 Hydraulic active heave compensation system – modelling and simulation

2.1. Modelling of the electrohydraulic servo drive with a hydraulic cylinder

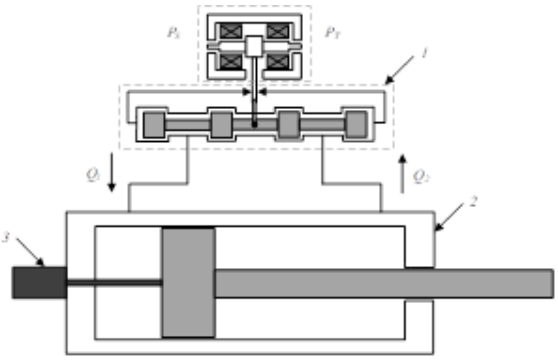

Fig. 1. Scheme of the electrohydraulic servo drive with a hydraulic cylinder.

* Corresponding author: arkadiusz.z.jakubowski@doctorate.put.poznan.pl

The first electrohydraulic servo drive consists of a servo valve *1* and a hydraulic actuator *2*. The servo valve is connected to the hydraulic cylinder as shown on Fig. 1. The actual position of a hydraulic cylinder piston (double acting cylinder) is measured via a displacement sensor *3*.

Scheme of the four edge electrohydraulic amplifier is shown on Fig.2.

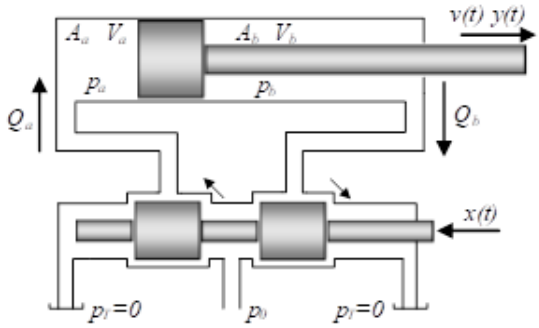

Fig. 2. Scheme of the four-edge electrohydraulic amplifier with a hydraulic actuator.

The equations describing the electrohydraulic servo drive model with a hydraulic actuator can be specified as follows [11, 12]:

$$Q_a(t) = Q_{sa}(t) + Q_{ha}(t) + Q_v(t) \tag{1}$$

$$Q_b(t) = Q_{sb}(t) + Q_{hb}(t) - Q_v(t) - Q_{vb}(t) \tag{2}$$

$$Q_a(t) = K_{Qp}x(t) - K_l[p_0 - p_a(t)] \tag{3}$$

$$Q_b(t) = K_{Qp}x(t) - K_l p_b(t) \tag{4}$$

$$Q_{ha}(t) = A\frac{dy(t)}{dt}, \quad Q_{hb}(t) = aA\frac{dy(t)}{dt} \tag{5}$$

$$Q_{sa}(t) = \frac{V_a}{E_o}\frac{dp_a(t)}{dt}, \quad Q_{sb}(t) = -\frac{V_b}{E_o}\frac{dp_b(t)}{dt} \tag{6}$$

$$Q_v(t) = K_v[p_a(t) - p_b(t)] \tag{7}$$

$$Q_{vb}(t) = K_{vb}p_b(t) \tag{8}$$

$$m\frac{d^2y(t)}{dt^2} + D\frac{dy(t)}{dt} = A[p_a(t) - ap_b(t)] \tag{9}$$

where: Q_a, Q_b – flow, Q_{ha}, Q_{hb} – absorption of the actuator chambers, Q_{sa}, Q_{sb} – flow of the covering losses due to compressibility, Q_{vb} – leakage flow on the piston rod, p_a, p_b – the pressure in the chambers of the actuator, A_a, A_b – active surfaces of the piston, V_a, V_b – the volume of liquid in the chambers of the actuator.

2.2 Modelling of the electrohydraulic servo drive with a hydraulic motor

The second electrohydraulic servo drive consists of a servo valve *1* and a hydraulic motor *2*. The servo valve is connected to the hydraulic motor as shown on Fig. 3. The actual position of the hydraulic motor is measured by an incremental encoder *3*.

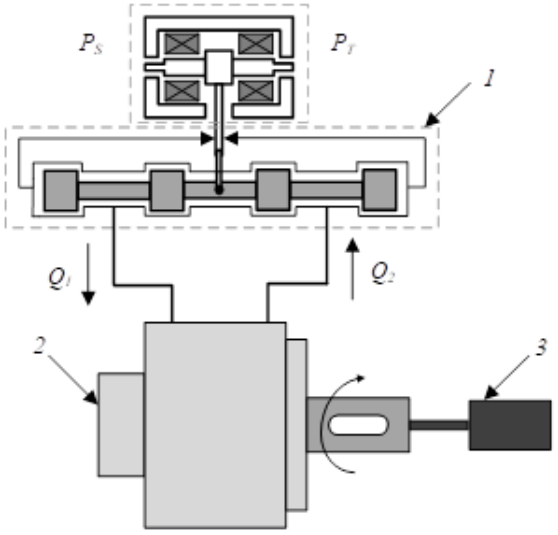

Fig. 3. Scheme of the electrohydraulic servo drive with a hydraulic motor.

The parameters of a hydraulic motor are needed for its modelling. The equations below are used to determine these parameters:

$$n_m = Q_t / V_m \tag{10}$$

$$\Delta P = \frac{2\pi}{V_m}T \tag{11}$$

where: n_m – motor speed, ΔP – applied pressure differences, V_m – geometric volume of motor, T – loading torque, Q_t – theoretical flow rate.

The theoretical motor flow rate is smaller than the real flow due to the internal leakage. The volumetric efficiency of the motor can be specified as follows:

$$\eta_v = \frac{Q_t}{Q} \tag{12}$$

or

$$n_m = \frac{Q\eta_v}{V_m} \tag{13}$$

The output mechanical power of the motor is smaller than the input hydraulic power. The power losses are evaluated by the total efficiency η_t:

$$Q\Delta P\eta_T = 2\pi n_m T \tag{14}$$

then:

$$\Delta P = \frac{2\pi}{V_m \eta_m \eta_h} T \tag{15}$$

where: Q – real motor flow, η_T– total motor efficiency η_m – motor mechanical efficiency, η_v – motor volumetric efficiency, η_m – motor hydraulic efficiency.

The mathematical model of the hydraulic motor describes its dynamics. The equations below describe the hydraulic motor [13, 14].

$$\dot{\omega}_k = J_m^{-1}[q_m f(q)(p_i - p_j) - (M_l / u_{mech} + b_\omega \omega_k + b_p |p_i - p_j| \cdot sign\,\omega_k + b \cdot sign\,\omega_k)] \tag{16}$$

$$\dot{\varphi}_k = \omega_k \tag{17}$$

$$Q_{i,j} = q_m f(q) \omega_k \pm k_{lea} p_{i,j} \tag{18}$$

where: ω_k – angular speed of the hydraulic motor shaft, J_m – moment of inertia, q_m – maximal geometric volume, $f(q)$ – parameter of regulation: $-1 \leq f(q) \leq 1$, M_l – loading moment, b_ω, b_p, b– coefficients of the hydraulic motor hydro mechanical losses, u_{mech} – transfer number of the working mechanism gear, k_{lea} – coefficient of the hydraulic motor volumetric losses.

3 Simulation

The simulation model was built based on the Simulink SimHydraulics tool. In Fig. 4 the simulation model of the electrohydraulic servo drive with a hydraulic cylinder is shown. The stroke of the double acting hydraulic cylinder was equal to 400 mm. The diameters of the piston and piston rod were respectively 60 mm and 100 mm. The value of the reduced mass was equal to 37, 3 kg (mass of the piston, piston rod and hydraulic motor, intermediate plate which is fixed at the end of piston rod).

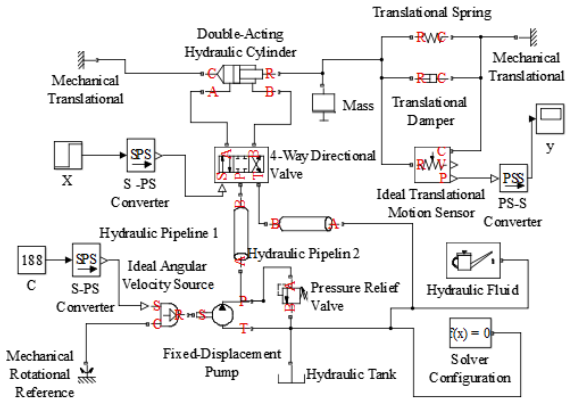

Fig. 4. Model of the hydraulic cylinder in Mathlab Simulink software.

The step response model of a hydraulic cylinder was checked by the Authors. Fig. 5 shows the simulation results with displacement of the piston rod. The simulation was performed for the supply pressure p_o equal to 5 MPa, 10 MPa and 15 MPa.

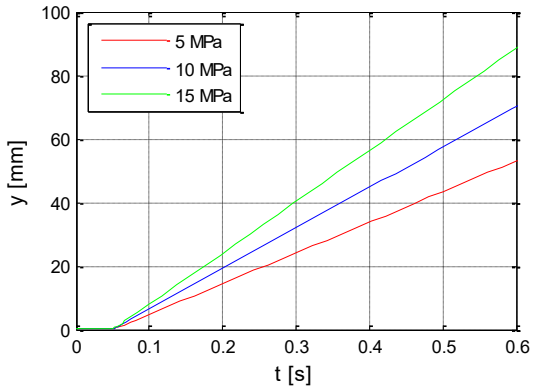

Fig. 5. Displacement of the piston road for a supply pressure of 5 MPa, 10 MPa and 15 MPa.

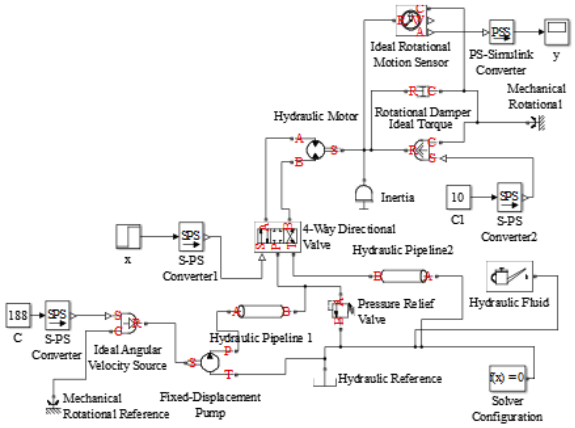

Fig. 6. Model of the hydraulic motor in Mathlab Simulink software.

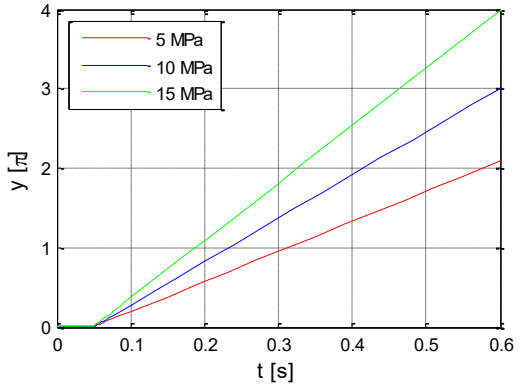

Fig. 7. Displacement of the shaft hydraulic motor for a supply pressure of 5 MPa, 10 MPa and 15 MPa.

In Fig. 6 the simulation model of the electrohydraulic servo drive with a hydraulic motor is shown. A steel load was fixed to the hydraulic motor via a steel cable. Mass of the steel load was equal to 5 kg.

The model of the electrohydraulic servo drive with a hydraulic cylinder and a hydraulic motor was tested by the step response signals. Fig. 7 shows the simulation results for the hydraulic motor shaft position. The model of the hydraulic motor was tested for different supply pressures such as: 5 MPa, 10 MPa and 15 MPa.

4 Experimental research

The electrohydraulic servo drives were tested by the Authors. In Fig. 8 the test stand is presented. The test stand consists of a hydraulic cylinder with a stroke range of 400 mm. The hydraulic cylinder is used for waves simulation. At the end of the piston rod the hydraulic motor with a maximum rotary speed range of 810 rpm is fixed. Maximum output power of the hydraulic motor was equal to 16 kW. The hydraulic cylinder and hydraulic motor were combined with servo valves. The hydraulic cylinder was equipped with the displacement sensor. The actual position of the hydraulic motor was measured via an incremental encoder.

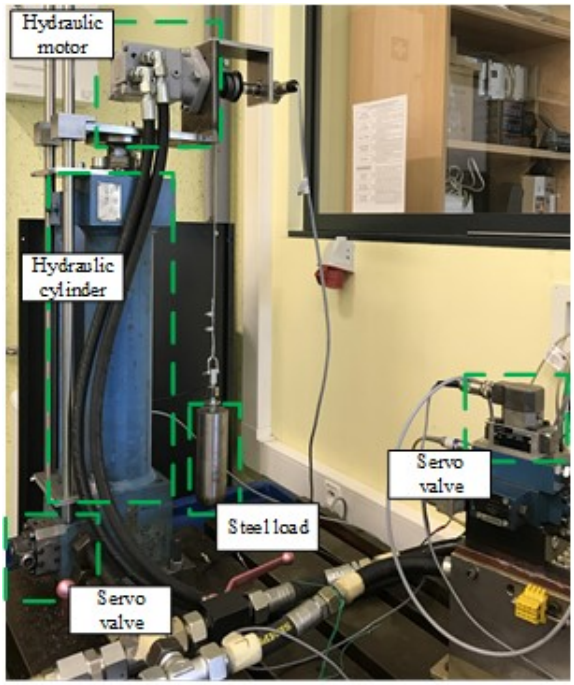

Fig. 8. The view of the test stand.

The hydraulic power supply used by the Authors is characterized by the following parameters: maximum flow rate= 100 dm3/min, maximum pressure p_0 = 40 MPa, motor power = 37 kW, filtration at 6 microns. The last step was to test a real object and compare the step response simulation model and a real hydraulic cylinder and a hydraulic motor. The supply pressure for the tested hydraulic cylinder and hydraulic motor was equal to 10 MPa. In Fig. 9 the displacement piston rod (hydraulic cylinder) for a real object and a model is presented. In Fig. 10 the displacement of the shaft hydraulic motor is illustrated by the Authors.

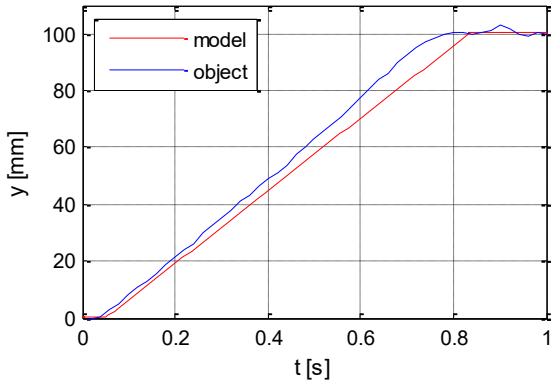

Fig. 9. Displacement of the piston rod for a model and a real object.

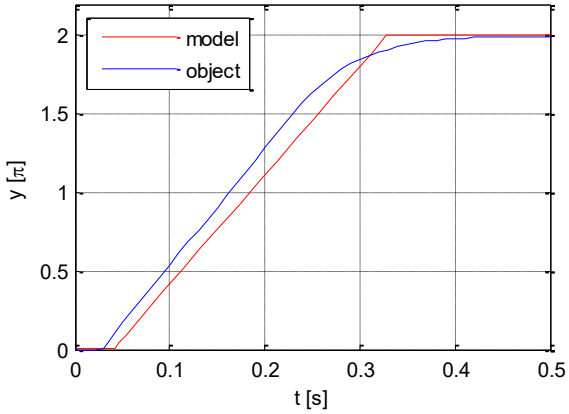

Fig. 10. Displacement of the shaft hydraulic motor for a model and a real object.

5 Conclusions

The article presents basic equations describing an electrohydraulic servo drive with a hydraulic cylinder and a hydraulic motor. The PLC was connected to the servo valves via dedicated control cards (valves amplifier). The simulation model was built by using the SimHydraulics tool. The hydraulic motor and hydraulic cylinder were controlled by the electrohydraulic servo valve. The test stand was built to compare the results of the simulation and the real objects. Further research aims to improve the simulation models of a hydraulic motor and a hydraulic cylinder.

The work described in this paper was funded from 02/22/DSMK/1408 (Sterowanie urządzeniami mechatronicznymi z zastosowaniem technik nieliniowych oraz bioelektrycznej aktywności mózgu).

References

1. J.S. Cundiff, *Fluid power circuits and controls* (CRC Press LLC, USA, 2002)
2. P. Chapple *Principles of hydraulic system design,* (Coxmoor , 2003)
3. J.K. Woodacre, R.J. Bauer, R.A. Irani, J. Phys. Conf. Ser. **104,** 140-154 (2015)

4. A.A. Walid, P. Gu, M.R. Hansen, G. Hovland, Y. Iskandarani, IJMECH. 291-296 (2011)
5. A. Huster, H. Bergstrom, J. Gosior, D. White, Wit. Trans. Ecol. Envir. 1-8 (2009)
6. J.T. Hatleskog, M.W. Dunningan, Wit. Trans. Ecol. Envir. 1-6 (2006)
7. L. Huang, Y. Zhang, L. Zhang, M. Liu, Petrol. Explor. Develop. **40(5),** 655-670 (2013)
8. J. Ni, S. Liu, M. Wang, X. Hu, Y. Dai, Appl. Mech. Mater. 5111-5116, (2009)
9. A. Kyllingstad, US. Patent 8,265,811 (2012)
10. S. Kuchler, T. Mahl, J. Neupert, K. Schneider, O. Sawodny, Trans. of Mechatronics. **16.2,** 297-309 (2011)
11. A. Milecki, D. Rybarczyk, Stroj. Vestn-J. Mech. E. **61(9)**, 517-522 (2015)
12. D. Rybarczyk, D. Sędziak, P. Owczarek, A. Owczarkowski, *Progress in Automation, Robotics and Measuring Techniques*, 215-222 (2015)
13. E.Y. Malinovsky, L.B. Zaretsky, Y.G. Berengard, M.M. Gaitsgori, PJSC. (1980)
14. I.I. Bazhin, Y.G. Berengard, M.M. Gaitsgori, PJSC. (1988)